2nd Department of Radiology, Medical University of Lublin

MAREK PASŁAWSKI, KONRAD KRZYŻANOWSKI,
JANUSZ ZŁOMANIEC

Dissecting aortic aneurysm in spiral CT examination. MIP and VRT reconstructions

Acute aortic dissection (AAD) is one of the most dramatic cardiovascular emergencies. To limit the possibility of death, a detailed morphologic and functional diagnosis must be quickly obtained. Aortography has been the traditional method of assessing suspected AAD; however, concern over the low sensitivity of aortography has prompted the investigation of other imaging techniques for this purpose. Transesophageal echocardiography and magnetic resonance (MR) imaging are increasingly used in the evaluation of AAD and have sensitivities and specificities of 95%–100%. A recent study found that the sensitivity and specificity of helical computed tomography (CT) compare well with those of MR imaging and transesophageal echocardiography (5,6,7).

The aim of the study was to present the usefulness of the spiral CT examination with spatial reconstructions in assessment of the aortic dissection.

MATERIAL AND METHODS

Material comprises a group of 9 patients with aortic dissection, in whom spiral CT examination was performed. The examination begins with conventional unenhanced CT. Discontinuous images are obtained every 20 mm with 10-mm collimation in single mode; coverage begins 2 cm above the aortic arch and continues to the superior aspect of the femoral head. Unenhanced CT scans are useful in diagnosis of acute hemorrhage (pleural, mediastinal, or pericardial) and intramural hematoma, which are visualized as fluid collections of high attenuation (>50 HU), a finding consistent with fresh blood. We then inject 130 mL of nonionic contrast agent (Ultavist) at a rate of 3.5 mL/sec through a catheter positioned in the right arm. Helical CT is performed when desired enhancement in the aorta is obtained with the following parameters: 140 mA, 130 kV, pitch of 1.5, 3 mm collimation, and 3-mm reconstruction interval. Coverage begins 2 cm above the aortic arch and continues to the bifurcation of the iliac artery. Multiplanar reformation (MPR) images in sagittal, coronal, oblique sagittal and curved projections are generated. Maximum-intensity projection, shaded surface display (SSD) and volume rendered technique (VRT) reconstruction images of the target areas are also produced.

RESULTS

Standford type B aortic dissection was found in 7 patients. In on of them the intimal flap calcification enables diagnosis even on unenhanced images (Fig. 1A). Enhanced images reveal contrast flow in both, false and true aortic lumen (Fig. 1B). The MPR, MIP and VRT images reveal the intimal flap on the whole length (Fig. 2ABC). On VRT images closed end of the false lumen was easily seen (Fig. 3).
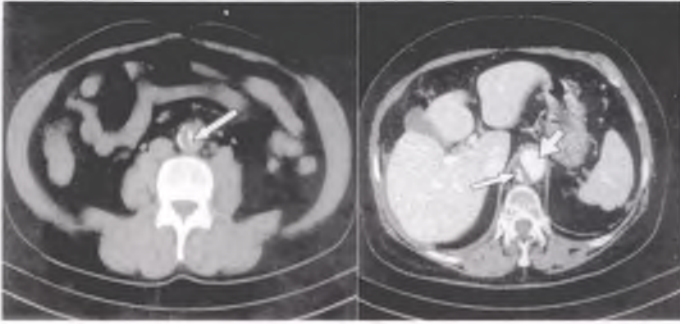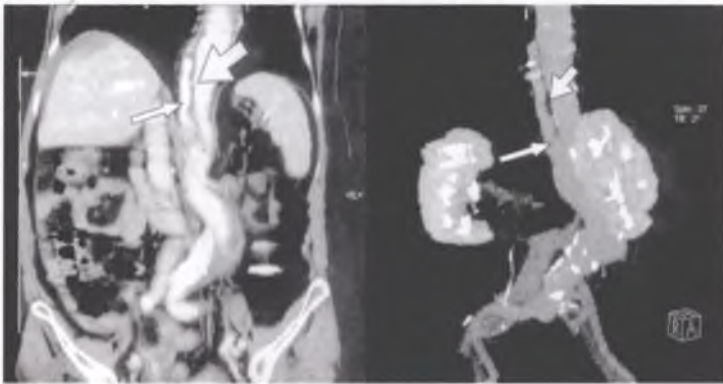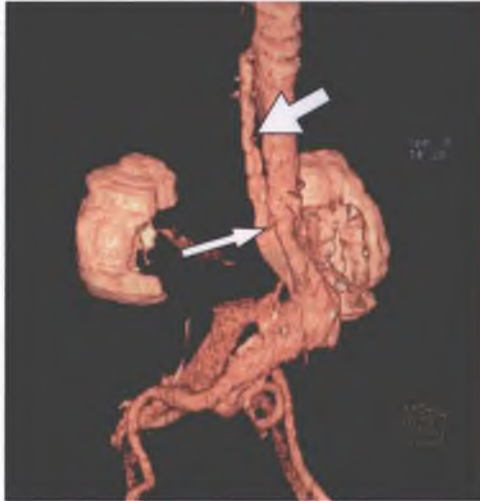
Fig. 1. Stanford type B aortic dissection. Unenhanced CT scan shows an intimal flap with calcification in the descending aorta (arrow) – A. Enhanced scan shows contrast flow in both, true and false lumens (arrows) – B

A   B

C

Fig. 2. Stanford type B aortic dissection on MPR – A, MIP – B and VRT images – C. Intimal flap marked with thick arrow. False lumen marked with a thick arrow

Fig. 3. Stanford type B aortic dissection on VRT image. The closed end false lumen marked with an arrow

Fig. 4. Stanford type B aortic dissection; with intimal flap in the aorta extending to the celiac trunk – an arrow

In one patient the intimal flap extended to the celiac trunk, without evidence of its occlusion (Fig. 4). In one patient the occlusion of the left renal artery with renal infract was seen on axial images (Fig. 5).

In 2 patients the Standford type B aortic dissection was found. In one of them the intima flap in ascending aorta, aortic arch and descending aorta, extending to the brachiocephalic trunk was seen on both axial images, MPR and VRT images (Fig. 6 and 7).

Fig. 5. Stanford type B aortic dissection. Intimal flap – thin arrow. Closed left renal artery –
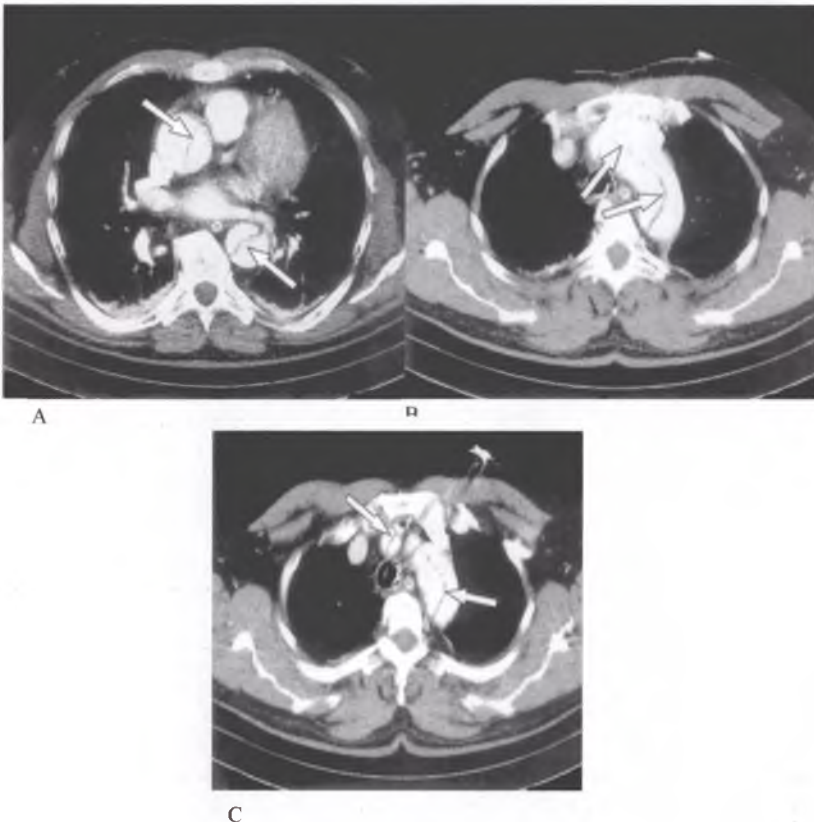a thick arrow. RI – renal infarct

Fig. 6. Stanford type A aortic dissection. Enhanced CT scans show an intimal flap (arrows)
in both, the ascending and descending aorta (A), in aortic arch (B) with extension
to the brachiocephalic trunk (C)

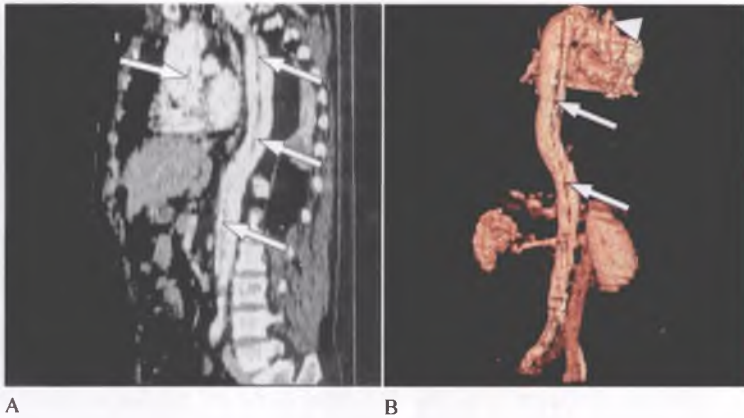A   B

Fig. 7. Stanford type A aortic dissection on MPR – A, and VRT images – B. Intimal flap marked with an arrow, visible in both ascending and descending aorta, with extension to the brachiocephalic trunk (arrowhead)

DISCUSSION

Various systems based on anatomic characteristics have been proposed to classify aortic dissection. The DeBakey classification consists of the following three types: I, both the ascending and the descending aorta are involved; II, only the ascending aorta is involved; and III, only the descending aorta is involved. The Stanford classification consists of the following two types: type A, involving the ascending aorta regardless of the entry site location; and type B, involving the aorta distal to the origin of the left subclavian artery. Many cases of aortic dissection do not fit into these classification schemes (3, 6).

The risk of acute aortic insufficiency, occlusion of the coronary vessels, or rupture of the dissection into the pericardium is extremely high (~90%) in type A dissection and necessitates immediate replacement of the aorta. This risk is lower in type B dissection, which can be controlled medically unless there is aortic rupture or renal or visceral vascular compromise. The dissection is termed *acute* when it is diagnosed within 14 days after the first symptoms appear; it is termed *chronic* when it is diagnosed later. Immediate appropriate treatment has improved the outcome of AAD: The overall inhospital mortality rate is currently less than 30%. Patients with aortic dissection require continuous surveillance. Residual aortic disease deteriorates into life-threatening conditions that require surgery in 15%–30% of patients after 10 years. Dilatation of the dissected region and progressive reduction of organ perfusion are the most frequent such conditions. In helical CT of AAD, it is important to evaluate the entire aorta to determine the distal extent of the dissection and to detect abdominal ischemic diseases that can increase the morbidity and mortality associated with this condition. Although primary reconstructed transverse sections remain the mainstay of CT angiographic interpretation, alternative visualization techniques, including multiplanar and three-dimensional reformation images, can substantially augment diagnosis and provide an efficient means of communicating critical anatomic relationships to referring clinicians (1, 3, 4, 6, 8).

Pain is the most common presenting symptom of aortic dissection. The pain of an aortic dissection is midline and is experienced in the front and back of the trunk, depending on the location of the dissection. The onset of pain is typically catastrophic, and it reaches a maximum level suddenly. The pain could be sharp, ripping, tearing, or knife-like in nature, but the abruptness is the most specific characteristic of the pain. Leg ischemia is one of the symptoms of aortic dissection (3, 8).

TYPICAL AORTIC DISSECTION

The classic feature of aortic dissection is a partition between the true and false channels; such a partition, which is formed by the intimal flap, is found in approximately 70% of cases. Secondary findings include internal displacement of intimal calcifications or a hyperattenuating intima; delayed enhancement of the false lumen; widening of the aorta; and mediastinal, pleural, or pericardial hematoma. In the Stanford classification, all dissections involving the ascending aorta are designated type A regardless of the site of the intimal tear or the distal extent of the dissection. Approximately 60% of aortic dissections are type A. There is general agreement that acute type A dissections require immediate surgical intervention. The most common complications are rupture of the dissection into the pericardium with progressive cardiac tamponade, occlusion of the coronary or supraaortic vessels, and severe aortic insufficiency with acute heart failure. The presence, location, and extent of an intimal flap may be readily determined with helical CT, but the technique is limited in assessment of coronary artery involvement and aortic insufficiency. Dissections involving any portion of the aorta distal to the left subclavian artery are designated type B in the Stanford classification. Approximately 40% of aortic dissections are type B (1, 2, 6).

H e l i c a l   C T   a r t i f a c t s . Most of the interpretive limitations of thoracic CT aortography are the result of two artifacts: perivenous streaks and aortic motion artifact. Perivenous streaks are caused by a combination of beam hardening and motion due to transmitted pulsation in a vein carrying undiluted contrast medium to the heart. In practice, perivenous streaks are rarely confused with aortic dissection because the orientation of such streaks typically varies from section to section and extend beyond the confines of the aortic wall. We minimize perivenous streaks by performing bolus injection into the right arm at a rate of 2 mL/sec. Aortic motion artifact simulates dissection of the ascending aorta and is related to movement of the aortic wall in the interval from the end of diastole to the end of systole. In most cases, the artifact is seen at the left anterior and right posterior margins of the aortic circumference and changes from one section to another. Use of a 180° linear-interpolation algorithm reduces the frequency of motion artifacts. When the findings on axial images are ambiguous, a serrated appearance of the left anterior ascending aorta on two- or three-dimensional reconstruction images provides clear evidence of a motion artifact (1, 6).

D i a g n o s t i c   p i t f a l l s . The CT appearances of several entities can cause they are mistaken for atypical AAD. A mural thrombus in a fusiform aneurysm; a focal periaortic soft-tissue mass such as periaortic fibrosis or a mediastinal, pulmonary, or retroperitoneal tumor; and anemia with apparent high attenuation of the aortic wall are examples of conditions that may be difficult to distinguish from AAD. The vascular structures around the aorta (aortic sinus, pericardial recess, left brachiocephalic vein, left superior intercostal vein) can also cause confusion (1, 6).

ATYPICAL AORTIC DISSECTION

I n t r a m u r a l   h e m a t o m a . Intramural hematoma (aortic dissection without rupture of the intima) is caused by hemorrhage of the vasa vasorum weakening the media without intimal tears. Intramural hematoma accounts for approximately 13% of all AADs. Unenhanced CT shows a cuff or crescent of high attenuation and displacement of intimal calcifications. On enhanced CT scans, a smooth region of low attenuation can be seen. In an open dissection, these features are difficult to differentiate from those of an acutely thrombosed false lumen. An observation that may help one differentiate intramural hematoma from the thrombosed false lumen of classic intimal dissection is that the latter entity tends to spiral longitudinally around the aorta, whereas the former entity tends to maintain a constant circumferential relationship with the aortic wall. Intramural hematoma of the ascending aorta has signs, symptoms, and a risk profile virtually identical to those of classic type A dissection and requires emergency surgical repair. Intramural hematoma can be detected and monitored with helical CT, MR imaging, and transesophageal echocardio-

graphy but not with aortography. It has been postulated that intramural hematoma is an early stage of classic aortic dissection; the prognosis is poor in cases that involve the ascending aorta (1, 6, 9).

Penetrating atherosclerotic ulcer. Penetrating atherosclerotic ulcer is defined as an atherosclerotic lesion with ulceration that penetrates the internal elastic lamina; such penetration facilitates hematoma formation within the media of the aortic wall. The appearance of this lesion is similar to that of a peptic ulcer on images from a barium study. Typically, penetrating atherosclerotic ulcer occurs in the middle or distal third of the thoracic aorta; CT features include a focal ulcer with adjacent subintimal hematoma (6).

Penetrating atherosclerotic ulcer can be differentiated from aortic dissection by means of (a) the extensive atherosclerotic disease and ectasia in penetrating atherosclerotic ulcer and (b) the lack of compression of the aortic lumen in elderly persons with penetrating atherosclerotic ulcer. Extension of the ulcer can produce incomplete rupture (adventitial false aneurysm) or transmural rupture. Penetrating atherosclerotic ulcer is treated by replacing the ulcerated area with a graft (6, 9).

Ruptured type B dissection. The CT features of aortic rupture include ire-gularrity of the aortic wall; extravasation of vascular contrast material; and hyperattenuating mediastinal, pericardial, or pleural fluid collections on unenhanced CT scans. These findings are consistent with mediastinal or pericardial hematoma or hemothorax. Most patients with type B AAD can be treated initially with medical therapy. The primary indications for immediate surgery are a ruptured aorta, a descending aortic diameter greater than 6 cm, malperfusion of the thoracoabdominal aorta, or pseudocoarctation syndrome with uncontrollable hypertension. The outcome seems to be worse in patients with retrograde involvement of the aortic arch and ascending aorta (1, 6).

Atypical configuration of the intimal flap. In some cases, the intimal flap has an atypical configuration. These atypical configurations are as follows: (a) dissection of the entire intima with a circumferential intimal flap; (b) a filiform (extremely narrow) true lumen, which can have ischemic complications; (c) a calcified false lumen in chronic dissection; (d) a three-channel aorta (Mercedes-Benz sign) or an aorta with several false channels; and (e) intimointimal intussusception (2, 6).

Associated diseases. Patients with hypertension or connective tissue disorders such as Marfan syndrome, cystic medial necrosis, Ehlers-Danlos syndrome, and Turner syndrome are at risk of aortic dissection. Pregnancy, aortic stenosis, bicuspid aortic valve, and aortic coarctation are other risk factors. In terms of symptoms, aortic dissection can mimic many other entities, including myocardial infarction, pericarditis, pulmonary thromboembolism, acute chole-cystitis, and inflammatory conditions involving the costochondral region. Moreover, a patient can have more than one of these diseases (3, 5, 6).

Postoperative complications of type A dissection. Surgical treatment of type A dissection consists of replacing the ascending aorta, reconstructing the aortic root to restore aortic valve competence, and directing blood flow preferentially to the true lumen. The mortality rate for surgical treatment of type A dissection is 10%–35%. Early postoperative complications include myocardial infarction, stroke, respiratory insufficiency, pulmonary embo-lism, aortic rupture, pseudoaneurysm, and graft infection (6). In a series of patients who underwent surgical repair of a type A dissection, the survival rate at 5 years was 95% when the false lumen was thrombosed and 76% when the false lumen was patent. At 10 years, 15%–30% of patients require surgery for life-threatening conditions such as dilatation of the dissected region with risk of rupture and progressive reduction of myocardial perfusion with development of severe aortic insufficiency (6).

Healing of intramural hematoma. Intramural hematomas can decrease in size and even disappear. An intramural hematoma of the descending aorta can be safely managed with observa-tion and does not necessarily require an early operation. Surgical intervention can be avoided if the hematoma resolves or if the symptoms disappear with negatively inotropic and hypotensive therapy. After several weeks, the hyperattenuating crescentic area on unenhanced CT scans becomes hypoattenuating (4, 6).

Progression of intramural hematoma. Although an intramural hematoma usually decreases in size, in some cases ulcerlike projections, an aneurysm, or open dissection develops in the affected segment of the aorta. Patients with intramural hematoma are at high risk of developing a saccular or fusiform aneurysm. Saccular aneurysms develop from ulcerlike projections (4, 6).

Aneurysm of the false lumen. One of the most significant findings during follow- up of an aortic dissection is an aneurysm of the false lumen. A complication of continuous dilatation of the false lumen is aortic rupture. Complete thrombosis and reduced flow in the false lumen decrease the risk of subsequent aortic dilatation. Elective resection is advisable if the aneurysm exceeds 5–6 cm in diameter or symptoms are present (6).

Aneurysm of the true lumen. Degenerative aneurysms associated with atheromatosis of the aorta most commonly involve the thoracic descending and abdominal segments. During follow-up of aortic dissection, an aneurysm of the true lumen can develop, particularly in older, hypertensive patients with advanced atherosclerosis of the intima. Surgery must be considered when the total aortic diameter reaches 6 cm (6).

ABDOMINAL COMPLICATIONS

Obstruction of abdominal branch vessels adds substantially to the mortality and morbidity rates in patients with aortic dissection and is a challenge to medical and surgical treatment of this disease. The frequency of such obstruction after AAD is as high as 27%. Infradiaphragmatic ischemic complications related to the main abdominal arterial branches (celiac trunk, superior mesenteric artery, main renal artery, and common iliac artery can be demonstrated in the arterial phase with our helical CT protocol. There are two types of branch-vessel occlusion. In static obstruction, the intimal flap intersects or enters the branch-vessel origin (3, 6).

Static obstruction is treated locally with an intravascular stent. In dynamic obstruction, the intimal flap spares the branch-vessel wall but prolapses across the branch-vessel origin and covers it like a curtain. Dynamic obstruction is treated with a fenestration procedure. In dynamic obstruction, the intimal flap has an ischemic configuration: The true lumen resembles a C-shaped envelope that is predominantly concave toward the false lumen. The presence of an ischemic configuration should be confirmed with manometry of the true and false lumina. Aneurysms of the abdominal branch vessels can be seen during follow-up of dissected vessels (3, 6).

Compromise of the celiac trunk and mesenteric artery. The celiac trunk and superior mesenteric artery almost invariably originate from the true lumen. Obstruction of the celiac trunk due to aortic dissection can lead to hepatic or splenic infarction. Obstruction of the mesenteric artery can lead to mesenteric ischemia. Clinical suspicion of mesenteric ischemia is based on the presence of abdominal pain, bloody diarrhea, recurrent sepsis, or elevated levels of hepatic or pancreatic enzymes. However, to establish the diagnosis of arterial compromise, there must be definite findings from manometry, intravascular ultrasound, or other radiologic studies (3, 6).

Compromise of the renal arteries. In assessment of aortic dissection, it is not uncommon to encounter extension of the intimal flap into the renal artery, particularly in

patients with acute azotemia. Nephrographic asymmetries can be caused by renal obstruction; however, they can also be caused by delayed delivery of contrast medium to a kidney predominantly supplied by the false lumen or by acute tubular necrosis due to transient ischemia that occurred early in the dissection process. Arteries supplied exclusively by the false lumen are rarely compromised. Demonstration of an ischemic configuration of the lumina is approximately 80% specific for a pressure deficit in branches that arise from the true lumen. Complete healing of renal artery dissection has been reported (1, 3, 6).

C o m p r o m i s e   o f   t h e   i l i a c   a r t e r i e s . Many type B aortic dissections demonstrate extension to the iliac arteries without clinical repercussions, but thrombosis or rupture of the iliac arteries can be seen. Clinical suspicion of lower extremity ischemia is based on the results of clinical examination of the legs; a confident diagnosis can be made with helical CT (3, 6, 8).

CONCLUSIONS

Helical CT can be used to study the entire aorta in AAD and for follow-up of chronic aortic dissection. This technique allows accurate diagnosis of the type of dissection, atypical forms of aortic dissection, and early and late complications after surgery or medical treatment. In addition, helical CT is useful in surveillance of abdominal branch-vessel compromise, which can be life threatening in the acute or chronic phase of aortic dissection. In most cases of aortic dissection, axial images are sufficient to demonstrate the presence, location, and extent of an intimal flap. MPR images provide an overall view of the aortic dissection and demonstrate the anatomic relationships between the flap and the adjacent great vessels. We prefer SSD images to maximum-intensity projection images for evaluation of complex three-dimensional relationships, particularly in regions of vessel overlap. SSD images can be produced in several colors and provide a more realistic three-dimensional view; thus, they are more easily understood by the vascular surgeon.

REFERENCES

1.   B a t r a P. et al.: Pitfalls in the diagnosis of thoracic aortic dissection at CT angiography. RadioGraphics, 20, 309, 2000.
2.   K a w a n o H. et al.: Thrombosed Stanford type A dissection of the aorta in an elderly patient following a fall. Internal Medicine, 44, 603, 2005.
3.   K h a n I.A. et al.: Clinical, diagnostic, and management perspectives of aortic dissection. Chest, 122, 311, 2002.
4.   M e s z a r o s I. et al.: Epidemiology and clinicopathology of aortic dissection A population-based longitudinal study over 27 years. Chest, 117,1271, 2000.
5.   N i e n a b e r C.A. et al.: Aortic dissection: New frontiers in diagnosis and management. Part I: From etiology to diagnostic strategies. Circulation,108, 628, 2003.
6.   S e b a s t i a C. et al.: Aortic dissection: Diagnosis and follow-up with helical CT. Radio-Graphics, 19, 45, 1999.
7.   S w i t z e r N.: The floating viscera sign. Radiology, 232, 244, 2004.
8.   T s u k a m o t o S. et al.: DeBakey IIIb aortic dissection originating in a distal aortic arch aneurysm. Ann. Thorac. Cardiovasc. Surg., 9, 209, 2003.
9.   Y o s h i d a S. et al.: Thoracic involvement of type A aortic dissection and intramural hematoma: Diagnostic accuracy— Comparison of emergency helical CT and surgical findings. Radiology, 228, 430, 2003.

SUMMARY

Acute aortic dissection (AAD) is one of the most dramatic cardiovascular emergencies. To limit the possibility of death, a detailed morphologic and functional diagnosis must be quickly obtained. Aortography has been the traditional method of assessing suspected AAD; however, concern over the low sensitivity of aortography has prompted the investigation of other imaging techniques for this purpose. Transesophageal echocardiography and magnetic resonance (MR) imaging are increasingly used in the evaluation of AAD and have sensitivities and specificities of 95%–100%. A recent study found that the sensitivity and specificity of helical computed tomography (CT) compare well with those of MR imaging and transesophageal echocardiography. The aim of the study was to present the usefulness of the spiral CT examination with spatial reconstructions in assessment of the aortic dissection. The material comprises a group of 9 patients with aortic dissection, in whom spiral CT examination was performed. The examination begins with conventional unenhanced CT. Discontinuous images are obtained every 20 mm with 10-mm collimation in single mode; coverage begins 2 cm above the aortic arch and continues to the superior aspect of the femoral head. Unenhanced CT scans are useful in diagnosis of acute hemorrhage (pleural, mediastinal, or pericardial) and intramural hematoma, which are visualized as fluid collections of high attenuation (>50 HU), a finding consistent with fresh blood. We then inject 130 mL of nonionic contrast agent (Ultavist) at a rate of 3,5 mL/sec through a catheter positioned in the right arm. Helical CT is performed when desired enhancement in the aorta is obtained with the following parameters: 140 mA, 130 kV, pitch of 1.5, 3 mm collimation, and 3-mm reconstruction interval. Coverage begins 2 cm above the aortic arch and continues to the bifurcation of the iliac artery. Multiplanar reformation (MPR) images in sagittal, coronal, oblique sagittal and curved projections are generated. Maximum-intensity projection, shaded surface display (SSD) and volume rendered technique (VRT) reconstruction images of the target areas are also produced. Standford type B aortic dissection was found in 7 patients. In one of them the intimal flap calcification enables diagnosis even on unenhanced images. Enhanced images reveal contrast flow in both, false and true aortic lumen. The MPR, MIP and VRT images reveal the intimal flap on the whole length. On VRT images not closed end of the false lumen was easily seen. In one patient the intimal flap extended to the celiac artery, without evidence of its occlusion. In one patient the occlusion of the left renal artery with renal infract was seen on axial images. In 2 patients the Standford type B aortic dissection was found. In one of them the intima flap in ascending aorta, aortic arch and descending aorta, extending to the brachiocephalic trunk was seen on both axial images, MPR and VRT images. Helical CT can be used to study the entire aorta in AAD and for follow-up of chronic aortic dissection. This technique allows accurate diagnosis of the type of dissection, atypical forms of aortic dissection, and early and late complications after surgery or medical treatment. In addition, helical CT is useful in surveillance of abdominal branch-vessel compromise, which can be life threatening in the acute or chronic phase of aortic dissection. In most cases of aortic dissection, axial images are sufficient to demonstrate the presence, location, and extent of an intimal flap. MPR images provide an overall view of the aortic dissection and demonstrate the anatomic relationships between the flap and the adjacent great vessels. We prefer SSD images to maximum-intensity projection images for evaluation of complex three-dimensional relationships, particularly in regions of vessel overlap. SSD images can be produced in several colours and provide a more realistic three-dimensional view; thus, they are more easily understood by the vascular surgeon.

Tętniak rozwarstwiający aorty w spiralnej tomografii komputerowej. Rekonstrukcje MIP i VRT

Ostre rozwarstwienie aorty jest stanem naglącym w medycynie. W celu ograniczenia śmiertelności szybka szczegółowa ocena morfologiczna i czynnościowa jest konieczna. Metody diagnostyczne obejmują aortografię, przezprzełykową ultrasonografię, rezonans magnetyczny i tomografię komputerową. Celem pracy jest przedstawienie użyteczności oceny spiralnej tomografii komputerowej z wykorzystaniem rekonstrukcji przestrzennych w ocenie rozwarstwie-

nia aorty. Materiał obejmuje grupę 9 pacjentów z rozwarstwieniem aorty, u których wykonano badanie TK. Badanie wykonano spiralnym tomografem komputerowym, w przekrojach grubości 2 mm, przed i po podaniu dożylnym środka kontrastowego strzykawką automatyczną. Oceniano obrazy osiowe, rekonstrukcje MPR, MIP oraz przestrzenne obrazy VRT. U siedmiu pacjentów stwierdzono tętniaka rozwarstwiającego typu B według Standforda. Zwapniała odwarstwiona błona wewnętrzna była widoczna na skanach niewzmocnionych. Na skanach po podaniu kontrastu uwidoczniono dwa kanały, prawdziwy i fałszywy. U jednego pacjenta rozwarstwienie obejmowało pień trzewny, u jednego miała miejsce niedrożność tętnicy nerkowej z zawałem nerki. U dwu pacjentów stwierdzono tętniaka typu A według Standforda. U jednego z nich widoczne było roz-warstwienie błony wewnętrznej obejmujące również pień ramienno-głowowy. Spiralna tomografia komputerowa jest bardzo skuteczną metodą obrazowania rozwarstwienia aorty. Zarówno skany osiowe, jak i rekonstrukcje MPR umożliwiają ocenę rozwarstwienia i jego rozległości. Rekon-strukcje MIP i przestrzenne obrazy VRT umożliwiają dokładną ocenę morfologii rozwarstwienia, jak też dodatkowych współistniejących zmian.